OXFORD CENTRE FOR COLLABORATIVE APPLIED MATHEMATICS

Report Number 11/13

Quasi-steady state analysis of two-dimensional random intermittent search processes

by

Paul C Bressloff and Jay M Newby

Oxford Centre for Collaborative Applied Mathematics
Mathematical Institute
24 - 29 St Giles'
Oxford
OX1 3LB
England

Quasi–steady state analysis of two–dimensional random intermittent search processes

Paul C. Bressloff[1,2] and Jay M. Newby[2]
[1] *Department of Mathematics, University of Utah, 155 South 1400 East, Salt Lake City UT 84112*
[2] *Mathematical Institute, University of Oxford, 24-29 St. Giles', Oxford, OX1 3LB, UK*

We use perturbation methods to analyze a two-dimensional random intermittent search process, in which a searcher alternates between a diffusive search phase and a ballistic movement phase whose velocity direction is random. A hidden target is introduced within a rectangular domain with reflecting boundaries. If the searcher moves within range of the target and is in the search phase, it has a chance of detecting the target. A quasi-steady state (QSS) analysis is applied to the corresponding Chapman-Kolmogorov (CK) equation. This generates a reduced Fokker-Planck (FP) description of the search process involving a non-zero drift term and an anisotropic diffusion tensor. In the case of a uniform direction distribution, for which there is zero drift and isotropic diffusion, we use the method of matched asymptotics to compute the mean first passage time (MFPT) to the target, under the assumption that the detection range of the target is much smaller than the size of the domain. We show that an optimal search strategy exists, consistent with previous studies of intermittent search in a radially-symmetric domain that were based on a decoupling or moment closure approximation. We also show how the decoupling approximation can break down in the case of biased search processes. Finally, we analyze the MFPT in the case of anisotropic diffusion, and find that anisotropy can be useful when the searcher starts from a fixed location.

PACS numbers: 05.40.-a,87.10.-e

I. INTRODUCTION

Random search strategies occur throughout nature as a means of efficiently searching large areas for one or more targets of unknown location, which can only be detected when the searcher is within a certain range. Examples include animals foraging for food or shelter, [1–4], the active transport of reactive chemicals in cells [5–7, 9, 10], a promoter protein searching for a specific target site on DNA [11–14], and the motor-driven transport and delivery of mRNA to synaptic targets along the dendrites of neurons [15–17]. One particular class of model, which can be applied both to foraging animals and active transport in cells, treats a random searcher as a particle that switches between a slow motion (diffusive) or stationary phase in which target detection can occur and a fast motion 'ballistic' phase; transitions between bulk movement states and searching states are governed by a Markov process [18–22]. Under the assumptions that the random search is unbiased and that the probability of finding a single hidden target is unity, it can be shown that there exists an optimal search strategy given by the durations of each phase that minimize the mean first passage time (MFPT) to find the target. Motivated by experimental observations of the motor–driven transport of mRNA granules in dendrites [23, 24], we recently extended a one–dimensional (1D) version of these models to the case of a directed intermittent search process, in which the motion is directionally biased and there is a non-zero probability of failing to find the target (due to competition with other targets or degradation) [16, 17]. In particular, we showed that there no longer exists an optimal search strategy unless additional constraints are imposed such as fixing the target hitting probability.

In the case of 1D intermittent search processes, in which the number of internal states of the searcher is sufficiently small, it is possible to derive analytical expressions for the MFPT and hitting probabilities by explicitly solving the backwards equation of the associated Chapman-Kolmogorov (CK) equations [16, 18, 19]. However, if the number of internal velocity states becomes large then some form of approximation is needed. For example, in higher spatial dimensions where the direction of motion is random, one can use a decoupling approximation between the second–order moments of the velocity distribution and the MFPT [20, 21]. One example where the number of internal states of the searcher can become large even in 1D is the molecular motor–based bidirectional transport of intracellular cargo along microtubule filaments. There is growing evidence that such transport is a result of the combined action of multiple motors attached to the cargo; the current velocity state is then determined by the subset of motors currently bound to the microtubule [25]. Microtubules are polarized filaments with biophysically distinct (+) and (−) ends, and this polarity determines the preferred direction in which an individual molecular motor moves. For example, kinesin moves towards the (+) end whereas dynein moves towards the (−) end. Thus, one possible mechanism for bidirectional transport is that groups of kinesin and dynein motors undergo a tug–of–war competition, where individual motors influence each other through the force they exert on the cargo [26–28]. We have recently analyzed a tug–of–war model of 1D random intermittent search, by carrying out a quasi–steady state (QSS) reduction of the corresponding CK equation [29]. The QSS reduction is based on the observation that the state transition rates of the searcher (motor-cargo complex) are fast compared to the velocities over a characteristic length scale. The reduced model is described by

a scalar Fokker–Planck (FP) equation, which can then be used to calculate the MFPT to find a target for a wide range of biophysically realistic motor transport models [30, 31].

In the case of axonal or dendritic transport in neurons, the microtubles tend to be aligned in parallel [32] so that one can treat the transport process as effectively 1D. On the other hand, intracellular transport within the soma of neurons and most non–polarized animal cells occurs along a microtubular network that projects radially from an organizing center (centrosome) with outward polarity [33]. This allows the delivery of cargo to and from the nucleus. Moreover, various animal viruses including HIV take advantage of microtubule-based transport in order to reach the nucleus from the cell surface and release their genome through nuclear pores [34, 35]. In contrast, the delivery of cargo from the cell membrane or nucleus to other localized cellular compartments will require a non–radial path involving several tracks. It has also been found that microtubules bend due to large internal stresses, resulting in a locally disordered network. This suggests that *in vivo* transport on relatively short length scales may be similar to transport observed *in vitro*, where microtubular networks are not grown from a centrosome and thus exhibit orientational and polarity disorder [10, 36]. A detailed microscopic model of intracellular transport within the cell would need to specify the spatial distribution of microtubular orientations and polarity, in order to specify which velocity states are available to a motor-cargo complex at a particular spatial location. However, a simplified model can be obtained under the "homogenization" assumption that the network is sufficiently dense so that the set of velocity states (and associated state transitions) available to the diffusing motor complex is independent of position. In that case, one can effectively represent the active transport and delivery of cargo to an unknown target within the cell in terms of a two– or three-dimensional random intermittent search model. This provides motivation for extending our previous QSS analysis to higher–dimensional search problems.

In this paper, we perform a QSS analysis of a two–dimensional (2D) random intermittent search process. We assume that all velocity states accessible to the searcher have the same speed v, but take the transition rates between the ballistic and search phases to depend on the particular direction θ of the velocity state. (In the case of active transport on an homogenized microtubular network, this could reflect a dependence of the binding/unbinding rates on the density of microtubules of different orientations). We first show how the QSS reduction leads to a FP equation with a nonzero advection or drift term and an anisotropic diffusion tensor (section II). In the special case that all velocity states are equally likely, we recover the random intermittent search model analyzed by Benichou *et. al.* [9, 20, 21], and the associated FP equation describes isotropic diffusion with zero drift. We then investigate the effectiveness of the QSS reduction by using the FP equation to calculate the MFPT to find the target in a bounded planar domain with reflecting external boundaries (section III). Under the further assumptions that the target disc is much smaller than the search domain and the search process is unbiased, we use matched asymptotics along the lines of Refs. [37–39] to calculate the MFPT as a function of model parameters, and compare our results with Monte Carlo simulations of the full model. As in previous studies of unbiased random intermittent search processes [9, 20, 21], there exists a global minimum of the MFPT as a function of the transition rates. An additional feature of our analysis is a comparison of the QSS approximation with the decoupling approximation of Benichou *et. al.*. One advantage of the QSS method is that it provides a systematic perturbation scheme that is applicable to a wide range of intermittent search models. Indeed, we show how the decoupling approximation breaks down in the case of biased search processes. On the other hand, the decoupling approximation generates a more analytically tractable expression for the MFPT in the case of unbiased search processes, which can then be used to calculate the global minimum. (In order to obtain sufficient numerical accuracy under the QSS approximation, it is necessary to include higher order terms in the asymptotic expansion).

II. RANDOM INTERMITTENT SEARCH MODEL

Consider a particle searching for a hidden target in the bounded planar domain $\Sigma = \{(x, y),\ 0 \leq x, y \leq L\}$, see Fig. 1. Within the interior of the domain Σ, the particle can exhibit two types of behavior: either Brownian motion with diffusion coefficient D_0 or ballistic motion with velocity $\mathbf{v}(\theta) = v(\cos\theta, \sin\theta)$ and $\theta \in [0, 2\pi)$. We assume that the target is at a fixed but unknown location $\mathbf{r}_0 = (x_0, y_0)$. If the particle is within a Euclidean distance ρ of the target and is in the diffusing phase, then the particle can detect or, equivalently, be absorbed by the target at a rate k. We also assume throughout that the target disc

$$\mathcal{U} = \{(x, y) \in \mathbb{R}^2 \| \sqrt{|x - x_0|^2 + |y - y_0|^2} \leq \rho\}$$

lies fully within the planar domain Σ, that is, $\mathcal{U} \subset \Sigma$. Transitions between the diffusing state and a ballistic state are governed by a discrete Markov process. The transition rate β from a ballistic state with velocity $\mathbf{v}(\theta)$ to the diffusive state is taken to be independent of θ, whereas the reverse transition rate is taken to be of the form $\alpha\mathcal{Q}(\theta)$ with $\int_0^{2\pi} \mathcal{Q}(\theta)d\theta = 1$.

Suppose that at time t the searcher is undergoing ballistic motion. Let $(X(t), Y(t))$ be the current position of the searcher and let $\Theta(t)$ denote the corresponding velocity direction. Introduce the conditional probability density $p(x, y, \theta, t)$ such that $p(x, y, \theta, t)dxdyd\theta$ is the joint probability that $(x, y, \theta) < (X(t), Y(t), \Theta(t)) <$

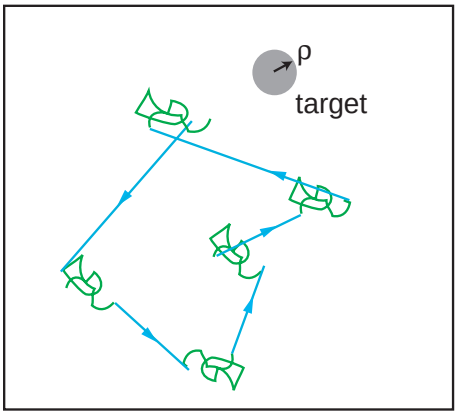

FIG. 1: Stochastic model of random intermittent search

$(x+dx, y+dy, \theta+d\theta)$ given that the particle is in the ballistic phase. Similarly, take $p_0(x,y,t)$ to be the corresponding conditional probability density if the particle is in the diffusive phase. For the moment we will leave the initial conditions unspecified. We then have the following Chapman–Kolmogorov (CK) equations describing the evolution of the probability densities for $t>0$:

$$\frac{\partial p}{\partial t} = -\nabla\cdot(\mathbf{v}(\theta)p) - \beta p + \alpha\mathcal{Q}(\theta)p_0 \tag{2.1}$$

$$\frac{\partial p_0}{\partial t} = D_0\nabla^2 p_0 + \beta\int_0^{2\pi} p(\mathbf{r},\theta',t)d\theta' - \alpha p_0 - k\chi(\mathbf{r})p_0, \tag{2.2}$$

with $\mathbf{r}=(x,y)$. The indicator function χ is defined according to

$$\chi(x,y) = \begin{cases} 1, & \text{if } (x,y)\in\mathcal{U} \\ 0, & \text{otherwise.}\end{cases} \tag{2.3}$$

Equations (2.1) and (2.2) are supplemented by reflecting boundary conditions along $\partial\Sigma$, that is, at $x=0,L$ and $y=0,L$. Note that in the case of a uniform density, $\mathcal{Q}(\theta)=1/(2\pi)$, equations (2.1) and (2.2) reduce to the random intermittent search model considered by Benichou *et. al.* [9, 20, 21].

Let $P(t)$ be the probability that the searcher has not found (been absorbed by) the target at time t. Thus,

$$P(t) = \int_\Sigma\left[\int_0^{2\pi} p(x,y,\theta,t)d\theta + p_0(x,y,t)\right]dxdy.$$

Integrating equations (2.1) and (2.2) with respect to $\mathbf{r},\theta$ shows that

$$\frac{dP}{dt} = -\int_\Sigma\nabla\cdot\left(\int_0^{2\pi}\mathbf{v}(\theta)p(\mathbf{r},\theta,t)d\theta\right)d\mathbf{r} + D_0\int_\Sigma\nabla^2 p_0(\mathbf{r},t)d\mathbf{r} - k\int_\Sigma\chi(\mathbf{r})p_0(\mathbf{r},t).$$

Using the divergence theorem, it follows that the probability flux through a point on the boundary $\mathbf{r}\in\partial\Sigma$ with outward unit normal $\hat{\mathbf{n}}$ is

$$J_0(\mathbf{r},t) = \left[\int_0^{2\pi}\mathbf{v}(\theta)p(\mathbf{r},\theta,t)d\theta - D_0\nabla p_0(\mathbf{r},t)\right]\cdot\hat{\mathbf{n}}, \tag{2.4}$$

so that the reflecting boundary condition is $J_0(\mathbf{r},t)=0$ for all $t>0$ and $\mathbf{r}\in\partial\Sigma$. It also follows that the total probability flux due to absorption by the target is

$$J(t) = k\int_{\mathcal{U}} p_0(x,y,t)dxdy, \tag{2.5}$$

where $\mathcal{U}$ is the target disc.

A. QSS reduction

In order to carry out a quasi steady–state (QSS) reduction of the CK equations (2.1) and (2.2), we first nondimensionalize by fixing the units of space and time according to $L=1$ and $L/v=1$. Furthermore, we assume that for the given choice of units, there exists a small parameter $\epsilon\ll 1$ such that all transition rates are $\mathcal{O}(\epsilon^{-1})$, the diffusivity $D_0=\mathcal{O}(\epsilon)$ and all velocities are $\mathcal{O}(1)$. Performing the rescalings $D_0\to\epsilon D_0$, $\alpha\to\alpha/\epsilon$ and $\beta\to\beta/\epsilon$, equations (2.1) and (2.2) become

$$\frac{\partial p}{\partial t} = -\nabla\cdot(\mathbf{v}p) - \frac{\beta}{\epsilon}p(\mathbf{r},\theta,t) + \frac{\alpha\mathcal{Q}(\theta)}{\epsilon}p_0(\mathbf{r},t) \tag{2.6}$$

$$\frac{\partial p_0}{\partial t} = \epsilon D_0\nabla^2 p_0 + \frac{\beta}{\epsilon}\int_0^{2\pi}p(\mathbf{r},\theta',t)d\theta' - \frac{\alpha}{\epsilon}p_0(\mathbf{r},t) - k\chi(\mathbf{r})p_0(\mathbf{r},t). \tag{2.7}$$

In the limit $\epsilon\to 0$, the system rapidly converges to the space-clamped (i.e. $\nabla p=\nabla p_0=0$) steady–state distributions $(p^{\rm ss}(\theta),p_0^{\rm ss})$ where

$$p_0^{\rm ss} = \frac{\beta}{\alpha+\beta}\equiv b, \quad p^{\rm ss}(\theta) = \frac{\alpha\mathcal{Q}(\theta)}{\alpha+\beta}\equiv a\mathcal{Q}(\theta). \tag{2.8}$$

The QSS approximation is based on the assumption that for $0<\epsilon\ll 1$, solutions remain close to the steady–state solution. Hence, we set

$$p(\mathbf{r},\theta,t) = u(\mathbf{r},t)p^{\rm ss}(\theta) + \epsilon w(\mathbf{r},\theta,t) \tag{2.9}$$

$$p_0(\mathbf{r},t) = u(\mathbf{r},t)p_0^{\rm ss} + \epsilon w_0(\mathbf{r},t), \tag{2.10}$$

where

$$u(\mathbf{r},t)\equiv\int_0^{2\pi}p(\mathbf{r},\theta,t)d\theta + p_0(\mathbf{r},t), \tag{2.11}$$

and

$$\int_0^{2\pi}w(\mathbf{r},\theta,t)d\theta + w_0(\mathbf{r},t) = 0. \tag{2.12}$$

Furthermore, we take the initial conditions to be

$$u(\mathbf{r},0)=\delta(\mathbf{r}-\mathbf{r}_0), \quad w(\mathbf{r},0)=w_0(\mathbf{r},0)=0, \tag{2.13}$$

which are equivalent to the following initial conditions for the full probability densities:

$$p(\mathbf{r},\theta,0)=\delta(\mathbf{r}-\mathbf{r}_0)p^{\rm ss}(\theta),\ p_0(\mathbf{r},0)=\delta(\mathbf{r}-\mathbf{r}_0)p_0^{\rm ss}. \quad (2.14)$$

Thus, we are assuming that the initial internal state of the searcher (diffusive or ballistic with velocity $\mathbf{v}(\theta)$) is generated according to the steady–state distributions $p^{ss}(\theta)$ and p_0^{ss}. In other words, the searcher starts on the slow manifold of the underlying dynamics. If this were not the case, then one would need to carry out a multiscale analysis in order to take into account the initial transient dynamics transverse to the slow manifold [40].

We can now use perturbation and projection methods to derive a closed equation for the scalar component $u(\mathbf{r},t)$. First, integrating equation (2.6) over θ and adding equation (2.7) yields

$$\begin{aligned}\frac{\partial u}{\partial t}&=\epsilon D_0\nabla^2 p_0-\langle\langle\mathbf{v}\cdot\nabla p\rangle\rangle-k\chi(\mathbf{r})p_0\\&=\epsilon bD_0\nabla^2u(\mathbf{r},t)-a\langle\mathbf{v}\rangle\cdot\nabla u-\epsilon\langle\langle\mathbf{v}\cdot\nabla w\rangle\rangle\\&\quad-k\chi(\mathbf{r})[bu+\epsilon w_0]+\mathcal{O}(\epsilon^2),\end{aligned} \quad (2.15)$$

where $\langle f\rangle=\int_0^{2\pi}\mathcal{Q}(\theta)f(\theta)d\theta$ and $\langle\langle f\rangle\rangle=\int_0^{2\pi}f(\theta)d\theta$ for any function or vector component $f(\theta)$. Next, substituting equations (2.9) and (2.10) into equations (2.6) and (2.7) yields

$$a\mathcal{Q}(\theta)\frac{\partial u}{\partial t}+\epsilon\frac{\partial w}{\partial t}=-\mathbf{v}(\theta)\cdot\nabla\left[a\mathcal{Q}(\theta)u+\epsilon w\right]-\beta w+\alpha\mathcal{Q}(\theta)w_0. \quad (2.16)$$

and

$$\begin{aligned}b\frac{\partial u}{\partial t}+\epsilon\frac{\partial w_0}{\partial t}&=\epsilon D_0\nabla^2\left(bu+\epsilon w_0\right)\\&\quad+\beta\langle w\rangle-\alpha w_0-k\chi(\mathbf{r})\left[bu+\epsilon w_0\right].\end{aligned} \quad (2.17)$$

Now substitute (2.15) into (2.16) and (2.17). Collecting terms to leading order in ϵ and using equation (2.12) then gives

$$w_0(\mathbf{r},t)\sim\frac{ab}{\alpha+\beta}\left[\langle\mathbf{v}\rangle\cdot\nabla u-k\chi(\mathbf{r})u\right], \quad (2.18)$$

and

$$\begin{aligned}w(\mathbf{r},\theta,t)\sim&\frac{\mathcal{Q}(\theta)}{\beta}\left(a^2(1+b)\langle\mathbf{v}\rangle-a\mathbf{v}(\theta)\right)\cdot\nabla u\\&+\frac{\mathcal{Q}(\theta)}{\beta}kab^2\chi(\mathbf{r})u.\end{aligned} \quad (2.19)$$

Finally, substituting equations (2.19), (2.18), (2.9) and (2.10) into (2.15) yields to $\mathcal{O}(\epsilon)$ the FP equation

$$\frac{\partial u}{\partial t}=-\nabla\cdot(\mathbf{V}u)+\epsilon bD_0\nabla^2u+\epsilon\nabla\cdot(\mathbf{D}\nabla u)-\lambda\chi(\mathbf{r})u. \quad (2.20)$$

The diffusion tensor $\mathbf{D}$ has components

$$\begin{aligned}D_{xx}&\sim\frac{a}{\beta}\left(\langle v_x^2\rangle-\langle v_x\rangle^2+b^2\langle v_x\rangle^2\right)\\D_{xy}&\sim\frac{a}{\beta}\left(\langle v_xv_y\rangle-\langle v_x\rangle\langle v_y\rangle+b^2\langle v_x\rangle\langle v_y\rangle\right)\\D_{yy}&\sim\frac{a}{\beta}\left(\langle v_y^2\rangle-\langle v_y\rangle^2+b^2\langle v_y\rangle^2\right),\end{aligned} \quad (2.21)$$

to lowest order in ϵ, whilst the effective drift velocity and detection rate are given by

$$\mathbf{V}\sim a\langle\mathbf{v}\rangle\left[1-\epsilon\frac{b\lambda_0\chi(\mathbf{r})}{\beta}\right] \quad (2.22)$$

$$\lambda\sim\lambda_0\left[1-\epsilon\frac{a\lambda_0}{\beta}\right],\quad \lambda_0=bk. \quad (2.23)$$

In the appendix we also calculate higher order contributions to the diffusion tensor $\mathbf{D}$ and detection rate λ. These higher order terms depend on $\chi(\mathbf{r})$ and will be needed in order to obtain sufficient numerical accuracy for our calculation of the MFPT to a small target, see section III. They are only nonzero inside the target domain because probability leaves the searching state at a rate k, which perturbs the solution away from the steady–state distribution. Thus, we can always take k small enough so that these extra terms are negligible. However, if the detection rate is large compared to the transition rates, the detection rate and diffusivity can be modified with enough higher order terms needed to reach the desired accuracy.

In the case of a uniform direction distribution $\mathcal{Q}(\theta)=1/(2\pi)$, the diffusion tensor reduces to a scalar. This follows from the fact that $v_x=v\cos\theta, v_y=v\sin\theta$ so $\langle v_x\rangle=\langle v_y\rangle=\langle v_xv_y\rangle=0$ and to leading order

$$D_{xx}=\frac{av^2}{2\beta}=D_{yy},\quad D_{xy}=0. \quad (2.24)$$

More generally, assuming that $\mathcal{Q}(\theta)$ is sufficiently smooth, we can expand it as a Fourier series,

$$\mathcal{Q}(\theta)=\frac{1}{2\pi}+\frac{1}{\pi}\sum_{n=1}^{\infty}(\omega_n\cos(n\theta)+\hat{\omega}_n\sin(n\theta)). \quad (2.25)$$

Assume further that $\omega_1=\hat{\omega}_1=0$ so there is no velocity bias i.e. $\langle v_x\rangle=\langle v_y\rangle=0$. Then

$$\begin{aligned}D_{xx}&=\frac{av^2}{\beta}\int_0^{2\pi}\cos^2(\theta)\mathcal{Q}(\theta)d\theta=\frac{av^2}{2\beta}(1+\omega_2)\\D_{yy}&=\frac{av^2}{\beta}\int_0^{2\pi}\sin^2(\theta)\mathcal{Q}(\theta)d\theta=\frac{av^2}{2\beta}(1-\omega_2),\\D_{xy}&=\frac{av^2}{\beta}\int_0^{2\pi}\sin(\theta)\cos(\theta)\mathcal{Q}(\theta)d\theta=\frac{av^2}{2\beta}\hat{\omega}_2.\end{aligned} \quad (2.26)$$

It follows that only the second terms in the Fourier series expansion contribute to the diffusion tensor.

Integrating the FP equation (2.20) over the planar domain Σ and using the divergence theorem shows that under the QSS approximation, the flux through the boundary reduces to

$$J_0(\mathbf{r},t)=[\mathbf{V}u(\mathbf{r},t)-\epsilon bD_0\nabla u(\mathbf{r},t)-\epsilon\mathbf{D}\nabla u(\mathbf{r},t)]\cdot\hat{\mathbf{n}}, \quad (2.27)$$

whereas the total flux into the target is

$$J(t) = \lambda \int_{\mathcal{U}} u(x,y,t)dxdy. \tag{2.28}$$

The form of these fluxes could also be obtained by substituting equations (2.9) and (2.10) into the rescaled versions of equations (2.5) and (2.5), and carrying out the appropriate perturbation expansion with respect to ϵ.

B. Backwards equation and MFPT

One of the main quantities of interest in random intermittent search processes is the MFPT to find the target, given that it started at position $\mathbf{r}$, which we denote by $T(\mathbf{r})$. Consistent with the QSS reduction, we assume that the initial internal state of the searcher is determined by the steady–state distributions $p^{ss}(\theta)$ and p_0^{ss}. The MFPT can be calculated directly in terms of the probability flux through the target according to [41]

$$T = \int_0^\infty tJ(t)dt. \tag{2.29}$$

One way to proceed would be to carry out the QSS approximation and then use Laplace transforms to solve the FP equation (2.20) with reflecting boundary conditions $J_0(\mathbf{r},t) = 0$ for all $\mathbf{r} \in \partial\Sigma$ and initial condition $u(\mathbf{r}',0) = \delta(\mathbf{r}'-\mathbf{r})$. This is the approach we took in our QSS analysis of 1D search problems [17, 29, 30]. In this paper, however, we will proceed by solving the corresponding backwards equation for the MFPT. First, note that under the QSS approximation the MFPT can be defined according to

$$T(\mathbf{r}) = \int_0^\infty U(\mathbf{r},t)dt, \quad U(\mathbf{r},t) = \int_\Sigma u(\mathbf{r}',t)d\mathbf{r}', \tag{2.30}$$

where $U(\mathbf{r},t)$ is the probability that the searcher hasn't been absorbed by the target at time t starting at position $\mathbf{r}$. It can be shown from equation (2.20) that U satisfies the backwards FP equation [41]:

$$\frac{\partial U}{\partial t} = \mathbf{V}\cdot\nabla U + \epsilon b D_0 \nabla^2 U + \epsilon \nabla\cdot(\mathbf{D}\nabla U) - \lambda\chi(\mathbf{r})U, \tag{2.31}$$

where we have used the fact that the diffusion tensor is symmetric. Integrating (2.31) with respect to time t and using the initial condition $U(\mathbf{r},0) = 1$, leads to the following backwards equation for the MFPT $T(\mathbf{r})$

$$-1 = \mathbf{V}\cdot\nabla T + \epsilon b D_0 \nabla^2 T + \epsilon \nabla\cdot(\mathbf{D}\nabla T) - \lambda\chi(\mathbf{r})T. \tag{2.32}$$

An alternative method for deriving equation (2.32) is to start from the backwards equations of the full CK system and then apply the QSS reduction to derive the corresponding backwards FP equation. That is, let $f(\mathbf{r},\theta,t)$ denote the conditional probability density that the searcher has not yet found the target at time t, given that it was initially at position $\mathbf{r}$ and had velocity $\mathbf{v}(\theta)$ at time $t = 0$. Similarly, let $f_0(\mathbf{r},t)$ denote the corresponding probability density assuming that the searcher was initially in a diffusing state. It is straightforward to show from equations (2.6) and (2.7) that f, f_0 satisfy the backwards CK equations [41]

$$\frac{\partial f}{\partial t} = \mathbf{v}\cdot\nabla f - \frac{\beta}{\epsilon}[f - f_0] \tag{2.33a}$$

$$\frac{\partial f_0}{\partial t} = \epsilon D_0 \nabla^2 f_0 + \frac{\alpha}{\epsilon}[\langle f\rangle - f_0] - k\chi(\mathbf{r})f_0. \tag{2.33b}$$

Under the QSS reduction, we decompose the solution as

$$f = U(\mathbf{r},t) + \epsilon z(\mathbf{r},\theta,t),\ f_0 = U(\mathbf{r},t) + \epsilon z_0(\mathbf{r},t), \tag{2.34}$$

with

$$U(\mathbf{r},t) \equiv a\,\langle f(\mathbf{r},\theta,t)\rangle + b f_0(\mathbf{r},t), \tag{2.35}$$

such that

$$a\,\langle z(\mathbf{r},\theta,t)\rangle + b z_0(\mathbf{r},t) = 0. \tag{2.36}$$

Proceeding along analogous lines to the QSS analysis of the forwards CK equations, we average equation (2.33a) with respect to the steady–state distribution $p^{ss}(\theta) = a\mathcal{Q}(\theta)$ and add the result to equation (2.33b) multiplied by $p_0^{ss} = b$. This gives

$$\frac{\partial U}{\partial t} = a\,\langle \mathbf{v}\cdot\nabla f\rangle + \epsilon b D_0\nabla^2 f_0 - \lambda_0\chi(\mathbf{r})f_0. \tag{2.37}$$

We then subtract the averaged equation (2.37) from equations (2.33a) and (2.33b) and then substitute for f, f_0 using equations (2.34). Collecting the leading order terms in ϵ and using equation (2.36) shows that

$$z_0 \sim -\frac{1}{\beta}\left[a\,\langle\mathbf{v}\rangle\cdot\nabla U + (k-\lambda_0)\chi(\mathbf{r})U\right] \tag{2.38}$$

and

$$z \sim \frac{1}{\beta}\left[\mathbf{v}(\theta)\cdot\nabla U - a(1+b)\,\langle\mathbf{v}\rangle\cdot\nabla U + b\lambda_0\chi(\mathbf{r})U\right]. \tag{2.39}$$

Finally, substituting equations (2.34) into equation (2.37) with z_0, z given by equations (2.38) and (2.39), we recover the backwards equation (2.31).

C. Decoupling approximation

An alternative method for generating a diffusion–like equation for the MFPT is presented by Benichou *et. al.* based on a so–called decoupling approximation [20]. This is essentially a moment closure approximation of the full system of equations for the MFPT. Defining $\mathcal{T}(\mathbf{r},\theta)$ to be the MFPT to find the target starting from a ballistic state of velocity $\mathbf{v}(\theta)$ and position $\mathbf{r}$, and $\mathcal{T}_0(\mathbf{r})$ to be the

corresponding MFPT starting in the diffusing state we have

$$\mathcal{T}(\mathbf{r},\theta)=\int_0^\infty f(\mathbf{r},\theta,t)dt,\quad T_0(\mathbf{r})=\int_0^\infty f_0(\mathbf{r},t)dt. \tag{2.40}$$

Integrating equations (2.33a) and (2.33b) with respect to time t and using the initial conditions $f(\mathbf{r},\theta,0)=f_0(\mathbf{r},0)=1$, then shows that

$$-1=\mathbf{v}(\theta)\cdot\nabla\mathcal{T}-\frac{\beta}{\epsilon}[\mathcal{T}-T_0] \tag{2.41}$$

$$-1=\epsilon D_0\nabla^2 T_0+\frac{\alpha}{\epsilon}[\overline{T}-T_0]-k\chi(\mathbf{r})T_0, \tag{2.42}$$

We also define the averaged quantities

$$\overline{T}(\mathbf{r})=\langle\mathcal{T}(\mathbf{r},\theta)\rangle\,,\quad \mathbf{\Theta}(\mathbf{r})=\langle\mathbf{v}(\theta)\mathcal{T}(\mathbf{r},\theta)\rangle\,. \tag{2.43}$$

We see from equation (2.30) that $\overline{T}$, T_0 and T are related according to $T(\mathbf{r})=a\overline{T}(\mathbf{r})+bT_0$. Averaging equation (2.41) with respect to the direction distribution $\mathcal{Q}(\theta)$ gives

$$-1=\nabla\cdot\mathbf{\Theta}-\frac{\beta}{\epsilon}(\overline{T}-T_0). \tag{2.44}$$

Similarly, multiplying equation (2.41) by $\mathbf{v}(\theta)$ and then averaging with respect to $\mathcal{Q}(\theta)$ gives

$$-\langle\mathbf{v}\rangle=\langle[\mathbf{v}\cdot\nabla\mathcal{T}]\mathbf{v}\rangle-\frac{\beta}{\epsilon}\mathbf{\Theta}+\frac{\beta}{\epsilon}\langle\mathbf{v}\rangle T_0. \tag{2.45}$$

Taking the divergence of this equation, we see that

$$\nabla\cdot\mathbf{\Theta}(\mathbf{r})=\frac{\epsilon}{\beta}\langle(\mathbf{v}\cdot\nabla)^2\mathcal{T}\rangle+\langle\mathbf{v}\rangle\cdot\nabla T_0. \tag{2.46}$$

We can obtain a closed set of equations for $\overline{T},T_0$ under the decoupling or moment–closure approximation [20]

$$\langle v_iv_j\mathcal{T}\rangle=\langle v_iv_j\rangle\langle\mathcal{T}\rangle=\langle v_iv_j\rangle\overline{T}. \tag{2.47}$$

Combining equations (2.44), (2.46) and (2.47) then leads to the equation

$$-1=\frac{\epsilon}{\beta}\langle(\mathbf{v}\cdot\nabla)^2\rangle\overline{T}+\langle\mathbf{v}\rangle\cdot\nabla T_0-\frac{\beta}{\epsilon}(\overline{T}-T_0). \tag{2.48}$$

Equations (2.48) and (2.42) form a closed pair of equations for $\overline{T},T_0$. In the case of unbiased search processes they reduce to the MFPT equations previously derived by Benichou *et. al.* [9, 20, 21].

In contrast to the QSS analysis, the domain of validity of the decoupling approximation is not specified . In particular, the decoupling approximation does not require *a priori* that the transition rates are relatively fast ($\epsilon\ll 1$). Nevertheless, we can check whether or not it is consistent with the QSS analysis in the small ϵ limit. For simplicity, suppose that $D_0=0$. We can then use equation (2.42) to express T_0 explicitly in terms of $\overline{T}$:

$$T_0(\mathbf{r})=\frac{\alpha}{\alpha+\epsilon k\chi(\mathbf{r})}\left(\overline{T}(\mathbf{r})+\frac{\epsilon}{\alpha}\right). \tag{2.49}$$

If (2.49) is now substituted into (2.48), we obtain the MFPT equation

$$-1=\widehat{\mathbf{V}}\cdot\nabla\overline{T}+\epsilon\nabla\cdot(\widehat{\mathbf{D}}\nabla\overline{T})-\widehat{\lambda}\chi(\mathbf{r})\overline{T} \tag{2.50}$$

with diffusion tensor $\mathbf{D}$ having components

$$\widehat{D}_{ij}=\frac{\alpha+\epsilon k\chi(\mathbf{r})}{\alpha+\beta+\epsilon k\chi(\mathbf{r})}\frac{1}{\beta}\langle v_iv_j\rangle \tag{2.51}$$

and

$$\widehat{\mathbf{V}}=\frac{\alpha+\beta}{\alpha+\beta+\epsilon k\chi(\mathbf{r})}a\langle\mathbf{v}\rangle\,,\quad \widehat{\lambda}=\frac{\alpha+\beta}{\alpha+\beta+\epsilon k\chi(\mathbf{r})}\lambda_0. \tag{2.52}$$

In the small ϵ limit, we recover the MFPT equation (2.32) of the QSS approximation with the same leading order drift term and detection rate, but the diffusion tensor $\mathbf{D}$ is replaced by $\widehat{\mathbf{D}}$. In the case of unbiased search processes ($\langle\mathbf{v}\rangle=0$), equations (2.21) and (2.51) imply that $\widehat{\mathbf{D}}\to\mathbf{D}$ as $\epsilon\to 0$ and, hence, the two approximation schemes have the same asymptotic limit. It has previously been shown that the decoupling approximation for unbiased search processes is accurate over a wide range of parameters that extends beyond the small ϵ regime [9, 20, 21]. This reflects the non-perturbative nature of this approximation with respect to ϵ. As we will illustrate in section III, it is necessary to include higher order terms in the QSS approximation in order to achieve a comparable level of numerical accuracy as ϵ increases.

In the case of biased search processes ($\langle\mathbf{v}\rangle\neq 0$), the decoupling approximation generates the incorrect asymptotic diffusion tensor. One possible source of this discrepancy is that the decoupling approximation does not generate the initial internal state of the searcher from the stationary solutions p_0^{ss} and $p^{ss}(\theta)$, since it involves equations for $\overline{T}(\mathbf{r})$ and $T_0(\mathbf{r})$ rather than $T(\mathbf{r})$. That is, in contrast to the QSS analysis, the searcher does not start on the slow manifold of the underlying time–dependent equations. As explained at some length in Ref. [40], this can lead to errors in any perturbation analysis even though the MFPT is itself approximately independent of the initial state in the small ϵ limit. In principle, one could modify the moment closure ansatz (2.47) in the case of biased search by taking

$$\langle v_iv_j\mathcal{T}\rangle=[c_1\langle v_iv_j\rangle+c_2\langle v_i\rangle\langle v_j\rangle]\overline{T}, \tag{2.53}$$

However, there does not appear to be a way to determine the coefficients c_1 and c_2 without introducing additional constraints along the lines of the QSS reduction, for example. It is also not clear how to generalize the decoupling approximation to the case of more complicated search models such as the "tug–of–war" model of motor–driven transport [30, 31].

III. MFPT TO A SMALL HIDDEN TARGET

We will now use the QSS approximation to calculate the MFPT to a target in the planar domain Σ. Note

that Benichou *et al.* previously analyzed a 2D intermittent search model using a simplified radially symmetric geometry with the target at the center of the disc [9, 20, 21]. In order to derive an analytical expression for the MFPT in the case of a planar domain, we will assume that the target is very small, that is, $\rho \ll L = 1$, and use matched asymptotic expansions. We will also assume that the search process is unbiased ($\langle \mathbf{v} \rangle = 0$), so that the decoupling and QSS approximations are consistent for sufficiently small ϵ, and set the diffusivity in the search state to zero, $D_0 = 0$.

A. Isotropic diffusion

We begin by considering the simpler case of isotropic diffusion and zero drift, which occurs when $\mathcal{Q}(\theta) = 1/2\pi$. The backwards equation (2.32) for the MFPT then becomes

$$-1 = D\nabla^2 T - \lambda\chi(\mathbf{r})T, \tag{3.1}$$

with

$$D \sim \frac{av^2}{2\beta} + \epsilon\frac{ab(1+b)kv^2}{2\beta^2}\chi(\mathbf{r}),\ \lambda \sim \lambda_0\left[1 - \epsilon\frac{a\lambda_0}{\beta}\right] \tag{3.2}$$

and reflecting boundary conditions $\partial_n T(\mathbf{r}) = 0$ for all $\mathbf{r} \in \partial\Sigma$. We have included the $\mathcal{O}(\epsilon)$ contribution to the diffusivity (see appendix). In order to obtain a solution that we can use to analyze the anisotropic case later on, we will take the planar domain Σ to be rectangular with height η_1 and width η_2 (in units of L). We will proceed by splitting the solution of the MFPT equation (3.1) into an interior problem within the target domain $\mathcal{U}$ and an exterior problem over the complementary domain $\Sigma/\mathcal{U}$. Since the target is small compared to the size of the domain (i.e. $\rho \ll 1$), we can assume that T is approximately constant around the boundary of the target $\partial\mathcal{U}$. In the exterior problem, we use matched asymptotics along the lines of Ref. [38] to solve in an inner region around $\mathcal{U}$ by ignoring boundary conditions on $\partial\Sigma$ and assuming a fixed (but unknown) value of T on $\partial\mathcal{U}$. The outer solution of the exterior problem is then found using the Neumann Green's function by treating the target as a source term.

To obtain the inner solution to the exterior problem, we introduce stretched coordinates $\mathbf{s}$ according to $\mathbf{r} = \mathbf{r}_0 + \rho\mathbf{s}$, where $\mathbf{r}_0$ is the center of the target disc of radius ρ, Setting $W(\mathbf{s}) = T(\mathbf{s}+\rho\mathbf{r}_0)$ and rescaling equation (3.1) gives

$$\begin{aligned} \nabla_s^2 W = 0, &\quad s \in \mathcal{U} \\ W = T_{\mathbf{r}_0}, &\quad \mathbf{s} \in \partial\mathcal{U}, \end{aligned} \tag{3.3}$$

where $T_{\mathbf{r}_0}$ is the unknown value of T on the target boundary. The solution, in terms of outer variables, has the far field behavior

$$W(\mathbf{r}) \sim T_{\mathbf{r}_0} + A\log|\mathbf{r} - \mathbf{r}_0| - A\log(\rho), \tag{3.4}$$

where A is an unknown constant. The outer solution to the exterior problem satisfies the equation

$$-1 = D_e\nabla^2 T, \quad \mathbf{r} \in \Sigma/\{\mathbf{r}_0\} \tag{3.5}$$

$$\partial_n T(\mathbf{r}) = 0, \quad \mathbf{r} \in \partial\Sigma \tag{3.6}$$

where the diffusivity, $D_e = \frac{av^2}{2\beta}$ is constant outside the target. This can be solved in terms of the Neumann Green's function, which satisfies

$$\nabla^2 G(\mathbf{r},\mathbf{r}') = \frac{1}{|\Sigma|} - \delta(\mathbf{r}-\mathbf{r}'), \quad r \in \Sigma \tag{3.7}$$

$$\partial_n G(\mathbf{r},\mathbf{r}') = 0, \quad \mathbf{r} \in \partial\Sigma \tag{3.8}$$

$$\int_\Sigma G(\mathbf{r},\mathbf{r}')dr = 0. \tag{3.9}$$

We solve the Green's function using separation of variables, and the result is expanded in terms of logarithms (see Appendix A for details):

$$G(\mathbf{r},\mathbf{r}') = \frac{1}{\eta_2}H_0(y,y') - \frac{1}{2\pi}\sum_{j=0}^{\infty}\sum_{n=\pm}\sum_{m=\pm}\left(\log|1-\tau^j z_n\zeta_m| + \log|1-\tau^j z_n\varsigma_m|\right), \tag{3.10}$$

where

$$\tau = e^{-2\pi\eta_1/\eta_2}, \quad z_\pm = \mathrm{e}^{i\pi(x\pm x')/\eta_2}, \quad \zeta_\pm = e^{-\pi|y\pm y'|/\eta_2}, \quad \varsigma_\pm = e^{-\pi(2\eta_1-|y\pm y'|)/\eta_2} \tag{3.11}$$

and

$$H_0(y,y') = \frac{\eta_1}{3} + \frac{1}{2\eta_1}(y^2 + y'^2) - \max\{y,y'\}, \tag{3.12}$$

Assuming that $\tau \ll 1$, we have the approximation

$$G(\mathbf{r},\mathbf{r}') = \frac{1}{\eta_2}H_0(y,y') - \frac{1}{2\pi}\sum_{n=\pm}\sum_{m=\pm}(\log|1-z_n\zeta_m| + \log|1-z_n\varsigma_m|) + \mathcal{O}(\tau). \tag{3.13}$$

The only singularity exhibited by equation (3.10) occurs when $\mathbf{r} \to \mathbf{r}'$, $\mathbf{r}' \notin \partial\Sigma$, in which case $z_- = \zeta_- = 1$ and the term $\log|1 - z_-\zeta_-|$ diverges. Writing

$$\log|1 - z_-\zeta_-| = \log|\mathbf{r} - \mathbf{r}'| + \log\frac{|1 - z_-\zeta_-|}{|\mathbf{r} - \mathbf{r}'|}, \quad (3.14)$$

where the first term on the right hand side is singular and the second is regular, we find that

$$G(\mathbf{r}, \mathbf{r}') = -\frac{1}{2\pi}\left(\log|\mathbf{r} - \mathbf{r}'| - R(\mathbf{r}, \mathbf{r}')\right), \quad (3.15)$$

where R is the regular part of the Green's function given by

$$\begin{aligned} R(\mathbf{r}, \mathbf{r}') = \frac{2\pi}{\eta_2}H_0(y, y') &- \log\frac{|1 - z_-\zeta_-||1 - z_-\zeta_+|}{|\mathbf{r} - \mathbf{r}'|} \\ &- \log|1 - z_-\varsigma_-||1 - z_-\varsigma_+| \\ &- \log|1 - z_+\varsigma_-||1 - z_+\varsigma_+| \\ &- \log|1 - z_+\zeta_-||1 - z_+\zeta_+| + \mathcal{O}(\tau). \end{aligned} \quad (3.16)$$

Using the Green's function, the outer solution to the exterior problem is

$$T(\mathbf{r}) = -\frac{|\Sigma|}{D_e}G(\mathbf{r}, \mathbf{r}_0) + T_{\text{av}}, \quad (3.17)$$

where $T_{\text{av}} = \int_\Sigma T(\mathbf{r})d\mathbf{r}$ is a constant. To determine the unknown constants A and T_{av}, we must match the inner and outer solution, which we do using the Van Dyke rule. Taking two terms of the outer solution and expanding to one term in inner variables yields

$$T(\mathbf{r}_0 + \rho\mathbf{s}) \sim \frac{|\Sigma|}{2\pi D_e}(\log|\rho\mathbf{s}| - R(\mathbf{r}_0, \mathbf{r}_0)) + T_{\text{av}}. \quad (3.18)$$

The first term of the inner solution, expanded to two terms in the outer variable is given by (3.4). After equating these two we get

$$A = \frac{|\Sigma|}{2\pi D_e}, \quad T_{\text{av}} = T_{\mathbf{r}_0} + \frac{|\Sigma|}{2\pi D_e}(R(\mathbf{r}_0, \mathbf{r}_0) - \log(\rho)). \quad (3.19)$$

Thus, the matched solution to the exterior problem is

$$\begin{aligned} T_e(\mathbf{r}) = T_{\mathbf{r}_0} &+ \frac{|\Sigma|}{2\pi D_e}\left(\log|\mathbf{r} - \mathbf{r}_0| - \log(\rho)\right) \\ &- \frac{|\Sigma|}{2\pi D_e}\left(R(\mathbf{r}, \mathbf{r}_0) - R(\mathbf{r}_0, \mathbf{r}_0)\right). \end{aligned} \quad (3.20)$$

The interior problem is given by

$$D_i\nabla^2 T_i - \lambda T_i = -1, \quad \mathbf{r} \in \mathcal{U}, \quad (3.21)$$

$$T_i(\mathbf{r}) = T_X, \quad \mathbf{r} \in \partial\mathcal{U}, \quad (3.22)$$

where from (3.2) the diffusivity inside the target is

$$D_i = \frac{av^2}{2\beta} + \epsilon\frac{av^2}{2\beta^2}(b+1)bk + \mathcal{O}(\epsilon^2). \quad (3.23)$$

We change to polar coordinates, $r = |\mathbf{r} - \mathbf{r}_0|$, with the target centered at the origin to get

$$D_i\nabla_r^2 T_i(r) - \lambda T_i(r) = -1, \quad 0 \le r < \rho \quad (3.24)$$

$$T_i(r) = T_{\mathbf{r}_0}, \quad r = \rho, \quad (3.25)$$

where ∇_r^2 is the standard radially-symmetric Laplacian. The solution to the homogeneous problem is well known in terms of the modified Bessel function I_n, and the solution to the inhomogeneous problem is simply $1/\lambda$. Thus, we have

$$T_i(r) = \left(T_{\mathbf{r}_0} - \frac{1}{\lambda}\right)\frac{I_0(\frac{r}{l_i})}{I_0(\frac{\rho}{l_i})} + \frac{1}{\lambda}, \quad (3.26)$$

where $l_i = \sqrt{D_i/\lambda}$ is the length scale associated with absorption in the target domain.

To match the interior solution (3.26) with the exterior solution (3.20), we impose conservation of flux along the boundary $\partial\mathcal{U}$. The flux at the boundary from the interior solution is

$$\left.\frac{\partial T_i}{\partial r}\right|_{r=\rho} = \left(T_{\mathbf{r}_0} - \frac{1}{\lambda}\right)\frac{1}{l_i}\frac{I_1(\frac{\rho}{l_i})}{I_0(\frac{\rho}{l_i})}. \quad (3.27)$$

Using (3.4), the flux at the target boundary from the exterior solution is

$$\left.\frac{\partial T_e}{\partial r}\right|_{r=\rho} = \frac{|\Sigma|}{2\pi D_e\rho}. \quad (3.28)$$

Equating (3.27) and (3.28) yields

$$T_{\mathbf{r}_0} = \frac{|\Sigma|l_i}{2\pi D_e\rho}\frac{I_0(\frac{\rho}{l_i})}{I_1(\frac{\rho}{l_i})} + \frac{1}{\lambda} \quad (3.29)$$

Thus, from equation (3.19), the full solution to the MFPT problem, averaged over the initial position is

$$T_{\text{av}} = \frac{1}{\lambda} + \frac{|\Sigma|}{2\pi D_e}\left(\frac{l_i}{\rho}\frac{I_0(\frac{\rho}{l_i})}{I_1(\frac{\rho}{l_i})} - \log(\rho) + R(\mathbf{r}_0, \mathbf{r}_0)\right) \quad (3.30)$$

and the solution, valid for starting positions $\mathbf{r}$ away from the target, is given by

$$T(\mathbf{r}) = \frac{1}{\lambda} + \frac{|\Sigma|}{2\pi D_e}\left(\frac{l_i}{\rho}\frac{I_0(\frac{\rho}{l_i})}{I_1(\frac{\rho}{l_i})} + \log|\mathbf{r}-\mathbf{r}_0| - \log(\rho) - (R(\mathbf{r},\mathbf{r}_0) - R(\mathbf{r}_0,\mathbf{r}_0))\right). \tag{3.31}$$

Fig. 2 shows a comparison of the QSS approximation of the MFPT given by (3.31) to averaged Monte-Carlo simulations as a function of the transition rates α and β (in physical units of s^{-1}). The QSS approximation is in good agreement with the numerics, provided that we include the $\mathcal{O}(\epsilon)$ corrections to the diffusivity and detection rate, see equation (3.2). Such terms are also necessary in order to identify a global minimum of the MFPT in the (α,β) plane. An example of such a minimum is illustrated in Fig. 3, which is in good agreement with numerical simulations and the corresponding MFPT calculated under the decoupling approximation. The latter is obtained by taking the diffusivity and detection rate to be determined from equations (2.51) and (2.52), see also section IIIB. A more detailed comparison of the two approximation schemes is presented in Fig. 4, where we plot the relative error with respect to Monte Carlo simulations. Interestingly, the QSS approximation is more accurate within a cone–like region of the (α,β)–plane, reflecting the asymptotic nature of the approximation. On the other hand, the accuracy of the decoupling approximation is more uniform with respect to parameter values, resulting in a slightly better approximation of the global minimum.

B. Optimal search strategy

The transition rates $\alpha_{\rm opt}$ and $\beta_{\rm opt}$ that minimize the MFPT determine an optimal random search strategy; these transition rates control the average time spent in the search and movement phases. We now calculate the optimal transition rates in the case of a small hidden target in a planar domain, following along similar lines to Benichou *et. al.* [9, 20, 21]. First, it is convenient to rewrite equations (3.30) and (3.31) in the more compact form

$$T = \frac{1}{\lambda} + \frac{|\Sigma|}{2\pi D_e}\left(g + \frac{1}{\rho}\sqrt{\frac{D_i}{\lambda}}\frac{I_0(\rho\sqrt{\frac{\lambda}{D_i}})}{I_1(\rho\sqrt{\frac{\lambda}{D_i}})}\right), \tag{3.32}$$

where g is independent of α,β. In the case of the space–averaged MFPT $T_{\rm av}$ we have

$$g = R(\mathbf{r}_0,\mathbf{r}_0) - \log(\rho), \tag{3.33}$$

whereas for arbitrary initial position $\mathbf{r}$,

$$g = \log|\mathbf{r}-\mathbf{r}_0| - \log(\rho) + R(\mathbf{r}_0,\mathbf{r}_0) - R(\mathbf{r},\mathbf{r}_0). \tag{3.34}$$

The MFPT depends on the transition rates via the diffiusivity D and effective detection rate λ, see equation (3.2). If the target is very easy to find, i.e. $\lambda \gg 0$, then there is no global minimum, since $T_{\mathbf{r}_0} \to 0$, see equation (3.29), and the MFPT is a monotonically decreasing function of $D_e = av^2/2\beta$; that is, $T \approx |\Sigma|g/2\pi D_e$. On the other hand, now suppose that the target is hard to find so that the length scale associated with target capture, $l_i = \sqrt{D_i/\lambda}$, is large compared to the radius ρ. Then, the Bessel functions can be approximated by

$$\frac{I_0(\rho\sqrt{\frac{\lambda}{D_i}})}{I_1(\rho\sqrt{\frac{\lambda}{D_i}})} \sim \frac{2}{\rho}\sqrt{\frac{D_i}{\lambda}}, \tag{3.35}$$

and the MFPT becomes

$$T \sim \frac{1}{\lambda\rho^2}\left(\frac{|\Sigma|}{\pi}\frac{D_i}{D_e} + \rho^2\right) + \frac{|\Sigma|g}{2\pi D_e}. \tag{3.36}$$

We can further simplify this expression using $\rho \ll 1$ to get

$$T \sim \frac{1}{\lambda}\left(\frac{|\Sigma|}{\pi\rho^2}\frac{D_i}{D_e}\right) + \frac{|\Sigma|g}{2\pi D_e}. \tag{3.37}$$

It turns out that the ratio D_i/λ is the critical quantity that allows the approximation to pick up the global minimum. In particular, higher order, k-dependent terms must be included in both the detection rate and the diffusivity. While the QSS approximation is capable of approximating the global minimum, we use the decoupling approximation in order to link up with previous studies of optimal intermittent search strategies. The result is a surprisingly accurate and simple formula for the optimal transition rates.

Suppose that we take the diffusivity D_i inside the target domain and detection rate λ to be given by the expressions obtained using the decoupling approximation, see equations (2.51) and (2.52):

$$D_e = \frac{av^2}{2\beta}, \quad D_i = \frac{\alpha+k}{\alpha+\beta+\epsilon k}D_e, \tag{3.38}$$

$$\lambda = \frac{\alpha+\beta}{\alpha+\beta+\epsilon k}\lambda_0. \tag{3.39}$$

Substitution into the MFPT (3.37) gives

$$T \sim \frac{|\Sigma|}{\pi\rho^2 k}\left(\frac{(\alpha+k)(\alpha+\beta)}{\alpha\beta}\right) + \frac{|\Sigma|g}{\pi v^2}\left(\frac{\beta(\alpha+\beta)}{\alpha}\right). \tag{3.40}$$

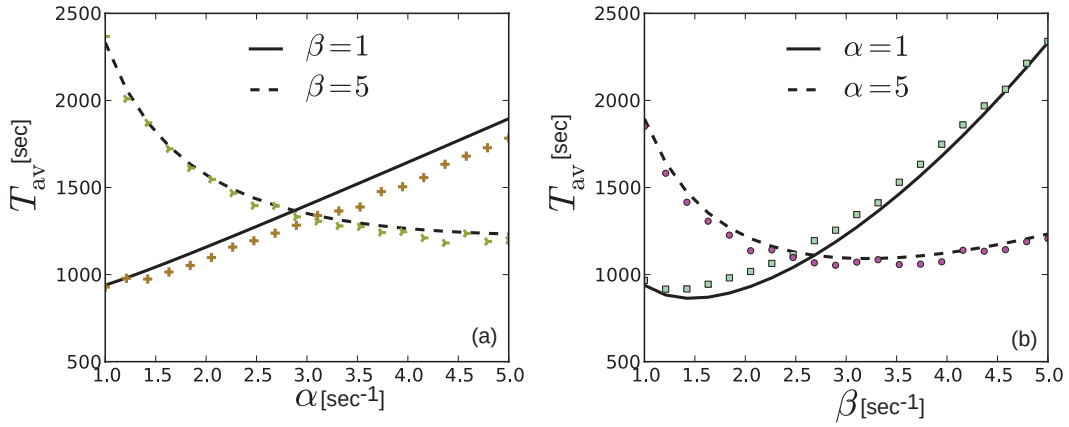

FIG. 2: The MFPT $T_{\rm av}$ of an unbiassed random intermittent search process on a square domain of length L. T is plotted as a function of (a) the transition rate α and (b) the transition rate β. The target is located at the center of the domain and the target radius is $\rho = 0.05L$. For the sake of illustration, $L = 10\mu m$, $v = 1\mu m s^{-1}$, $k = 0.5 s^{-1}$ and time is measured in seconds.

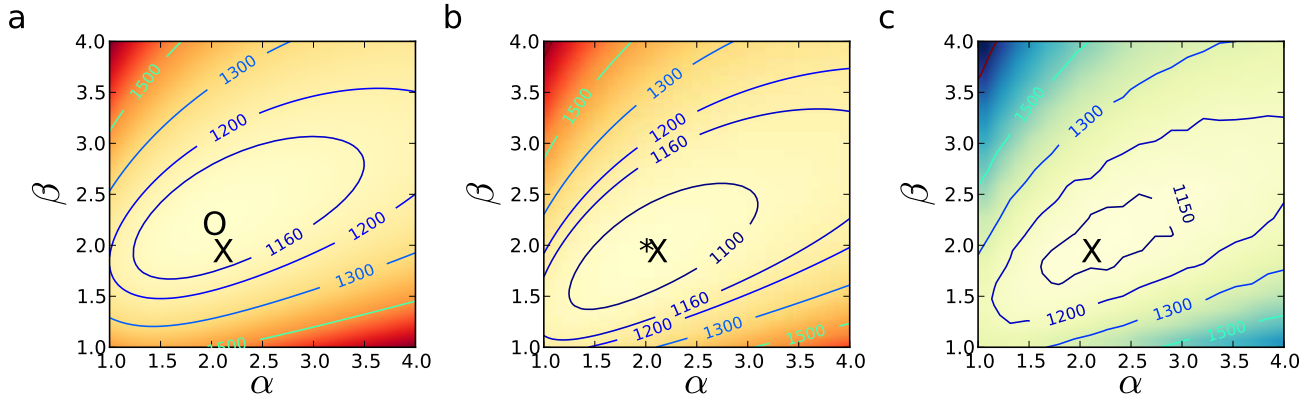

FIG. 3: Averaged MFPT, $T_{\rm av}$, in the (α, β) plane. a) Analytical approximation (3.30) with effective diffusivity and detection rate given by (3.2). The minimum is marked with an 'O' b) Decoupling approximation, with the minimum at $(\alpha_{\rm opt}, \beta_{\rm opt})$ marked with an '*' c) 10^5 averaged Monte-Carlo simulations for each value of (α, β) on a 20×20 grid. The minimum is marked by an 'X', which is also shown in (a,b) for comparison. Parameter values are $L = 10\mu m$, $\rho = 0.35\mu m$, $v = 1\mu m s^{-1}$, and $k = 1 s^{-1}$.

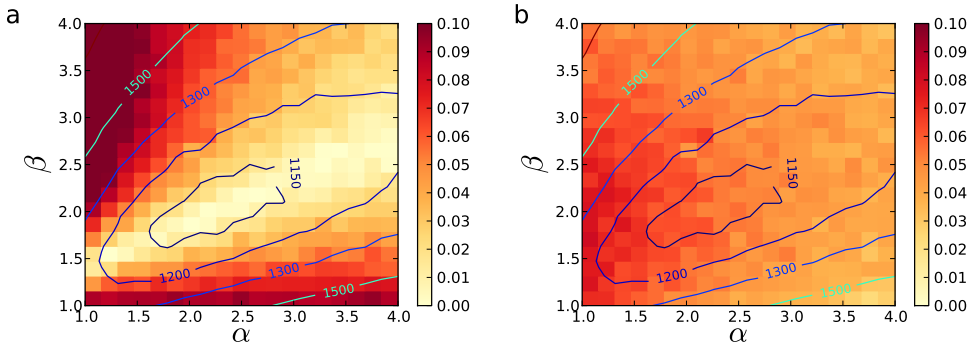

FIG. 4: Relative error for both approximations in Fig. 3 compared to Monte-Carlo simulations. The magnitude of the relative error is shown on the colorbar scale (dark red shows error greater than or equal to 0.1). Contours show the averaged MFPT from Monte-Carlo simulations in Fig. 3c. (a) The QSS reduction. The cone of accuracy reflects the asymptotic nature of the QSS approximation. (b) The decoupling approximation. The more uniform accuracy of the decoupling approximation give a slightly better estimate of the optimal transition rates, but the QSS approximation gives a slightly better estimate of the minimum MFPT.

Setting the partial derivatives $\frac{\partial T}{\partial \alpha}$ and $\frac{\partial T}{\partial \beta}$ to zero we have

$$\frac{|\Sigma| g}{\pi v^2}\frac{\beta^2}{\alpha^2} = \frac{|\Sigma|}{\pi \rho^2 k}\left(\frac{\alpha+k}{\alpha\beta} - k\frac{\alpha+\beta}{\alpha^2\beta}\right) \tag{3.41}$$

$$\left(\frac{|\Sigma|}{\pi\rho^2 k}\right)\frac{\alpha+k}{\beta^2} = \frac{|\Sigma| g}{\pi v^2}\left(1+\frac{2\beta}{\alpha}\right). \tag{3.42}$$

Rearranging then yields

$$\alpha^2 = \beta\left(k+\gamma\beta^2\right) \tag{3.43}$$

$$\gamma\beta^2\left(\alpha+2\beta\right) = (\alpha+k)\alpha, \tag{3.44}$$

where

$$\gamma = \frac{\rho^2 g k}{v^2}. \tag{3.45}$$

Solving (3.43) for α and substituting the result into (3.44) yields

$$\alpha = \sqrt{\beta(k+\gamma\beta^2)} \tag{3.46}$$

$$(\gamma\beta^2 - k)\left(\sqrt{\beta(k+\gamma\beta^2)}+\beta\right) = 0. \tag{3.47}$$

The real solutions to (3.47) are $\beta = 0$ and $\beta = \sqrt{\frac{k}{\gamma}}$. Thus, the unique optimal transition rates that minimize the averaged MFPT are

$$\alpha_{\text{opt}} \approx \left(\frac{2kv}{\rho}\right)^{1/2}\left(\frac{1}{R(\mathbf{r}_0,\mathbf{r}_0)-\log(\rho)}\right)^{1/4}, \tag{3.48}$$

$$\beta_{\text{opt}} \approx \frac{v}{\rho}\left(\frac{1}{R(\mathbf{r}_0,\mathbf{r}_0)-\log(\rho)}\right)^{1/2}, \tag{3.49}$$

$$\text{for } k=\mathcal{O}(1), \quad \rho \ll \sqrt{\frac{D_e}{\lambda}}, \quad \rho \ll 1, \quad \epsilon \ll 1.$$

By setting $R(\mathbf{r}_0,\mathbf{r}_0) = -1/2$ (the regular part of the Neumann Green's function for a circular domain, evaluated at $\mathbf{r}_0 = 0$ so that the target is located at the center) the above reduces to the result found in Ref. [20].

C. Anisotropic diffusion

For a general distribution of velocity directions $\mathcal{Q}(\theta)$, one must account for nonzero drift and an anisotropic diffusion tensor. In this section, we show how the results for the isotropic case can be modified to account for anisotropic diffusion when the drift term is zero. An anisotropic diffusion tensor can be eliminated from the problem using a coordinate transformation to a domain in which the diffusion is isotropic. The Green's function must then be calculated for the transformed domain, and the inner solution must be modified to account for a noncircular target domain.

As an example, consider an alternative to the random direction model, where the reorientations can occur in only one of four directions: up, down, left, or right. The corresponding direction distribution is

$$\mathcal{Q}(\theta) = \frac{q}{2}\left(\delta(\theta-\frac{\pi}{2})+\delta(\theta-\frac{3\pi}{2})\right) + \frac{(1-q)}{2}(\delta(\theta)+\delta(\theta-\pi)), \tag{3.50}$$

where $q \in (0,1)$ is a parameter that adjusts the anisotropy. For simplicity, we set $D_0 = 0$ and consider a square domain of size $L = 1$. After substituting (3.50) into the diffusion tensor (2.21), the MFPT equation (2.32) becomes

$$-1 = 2D\left(q\frac{\partial^2 T}{\partial x^2} + (1-q)\frac{\partial^2 T}{\partial y^2}\right) - \lambda\chi(x,y)T. \tag{3.51}$$

with reflecting boundaries on the unit square. Notice that when $q = 1/2$, the FP equation is identical to the isotropic model considered in the previous section.

Now, consider the coordinate transformation $\mathbf{r} \to \mathbf{z}$, where $\mathbf{z} = (\xi_1, \xi_2)$ and

$$\xi_1 = \frac{x}{\sqrt{2q}}, \quad \xi_2 = \frac{y}{\sqrt{2(1-q)}}. \tag{3.52}$$

The MFPT equation (3.51) is then transformed to (3.1) in the variable $\mathbf{z}$. Thus, the effect of anisotropy is equivalent to a distortion of the domain from the unit square to a rectangular domain with height $\eta_1 = (2(1-q))^{-1/2}$ and width $\eta_2 = (2q)^{-1/2}$ (see Fig. 5). Furthermore, the indicator function, $\tilde{\chi}(\mathbf{z})$, must now account for an elliptic target region.

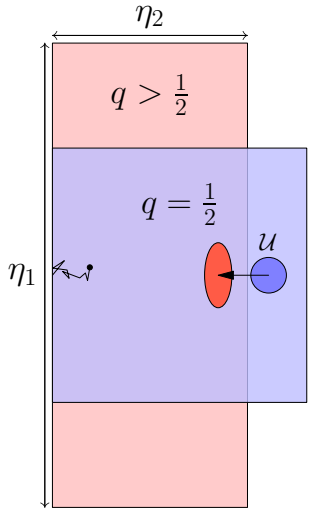

FIG. 5: Anisotropy in the diffusion tensor effectively alters the search domain. With no anisotropy (i.e. $q = 1/2$) the two domains are both the unit square (blue). As we increase q, diffusion in the y direction is inhibited, which effectively decreases the distance to the target, as seen in the rescaled domain (red).

One can show [37] that the Green's function (3.10) can be modified to deal with a noncircular target by scaling

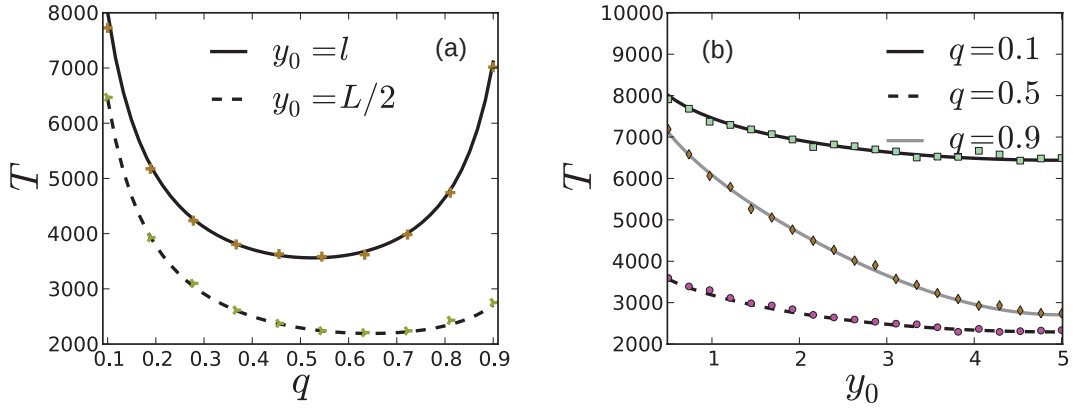

FIG. 6: Effect of anisotropy, q, on the MFPT as the target location $\mathbf{r}_0$ is varied whilst the initial position $\mathbf{r}$ of the searcher is fixed. (a) Plot of MFPT against q for various target locations. (b) Plot of MFPT against target location for various q. We take the $k \to \infty$ limit so that $\partial\mathcal{U}$ is an absorbing boundary. Domain parameters L and ρ are the same as in Fig. 2. The target location is $\mathbf{r}_0 = (L - 3\rho, y_0)$ with $\rho \leq y_0 \leq L/2$ and the initial position of the searcher is $\mathbf{r} = (0, L/2)$. Here $L = 10\mu m$ and $\rho = 0.5\mu m$. Transition rates are $\alpha = 4s^{-1}$ and $\beta = 6s^{-1}$ whilst the detection rate is $k = 0.5s^{-1}$.

the radius with the logarithmic capacitance $d_1 = \frac{1}{2}(\eta_1 + \eta_2)$ so that

$$G(\mathbf{r}, \mathbf{r}'; \rho) \to G(\mathbf{z}, \mathbf{z}'; d_1\rho). \tag{3.53}$$

The inner solution to the exterior problem and the solution to the interior problem must have the target radius rescaled so that the area of the effective circular target matches the area of the transformed elliptic target; that is, the matched value on $\partial\mathcal{U}$, given by (3.29), becomes

$$T_{\mathbf{r}_0}(\rho) \to T_{\mathbf{r}_0}(d_2\rho), \tag{3.54}$$

where $d_2 = \sqrt{\eta_1\eta_2}$. In Fig. 6, a comparison of the MFPT to averaged Monte-Carlo simulations is shown. The starting position is taken to be on the center of the left boundary ($\mathbf{r} = (0, L/2)$) and the position of the target is varied along the right boundary. As the anisotropy q is varied we see an optimal value that minimizes the MFPT.

IV. DISCUSSION

By combining the QSS reduction with the method of matched asymptotics for diffusion to a small target, we have developed a general analytical framework for studying random intermittent search processes. Indeed, with minor modifications one could consider higher spatial dimensions, multiple targets and splitting probabilities, and more complex transport models. The method proceeds by first applying the QSS reduction to obtain a FP equation for the probability density that approximates the random motion of the searcher. The MFPT to a hidden target is then approximated using matched asymptotics, under the assumption that the size of the target is small compared to the size of the domain. We applied our method to the particular example of a uniform direction distribution in the ballistic phase, for which the corresponding FP equation describes isotropic diffusion and zero drift. We assumed that the target was located in a rectangular domain so that the associated Green's function of the FP equation could be calculated exactly. (For more general geometries, a numerical boundary-integral method can be used [38]). Consistent with previous studies of random intermittent search processes [9, 20, 21], we established the existence of an optimal search strategy, where the transition rates that control the average time spent in the moving and searching phases are chosen to minimize the space-averaged MFPT, T_{av}, to the target. In order to achieve sufficient accuracy using the QSS approximation, it was necessary to include higher order corrections to the diffusivity and target detection rate of the associated FP equation. We also extended our analysis to the case of anisotropic diffusion and showed that anisotropy could be advantageous when the searcher starts from a fixed location.

One potential application of the analytical approach developed in this paper is to modeling mRNA transport within a developing drosophila embryo, where complex geometries and anisotropic diffusion along with specific target locations and initial conditions are all important factors. Experimental evidence also suggests the presence of weak directional bias and spatially inhomogeneous microtubule configurations [42, 43]. A key advantage of the QSS analysis is the ability to include spatially inhomogeneous transition rates and more complex internal state configurations, such as the tug-of-war model of motor transport [29–31].

Acknowledgements

This publication was based on work supported in part by the National Science Foundation (DMS-0813677) and

by Award No KUK-C1-013-4 made by King Abdullah University of Science and Technology (KAUST).

Appendix A

In this appendix we give details regarding how to construct the Neumann Green's function G defined by equations (3.7). We choose a particular representation that allows us to extract the regular part of the Green's function, following along similar lines to Ref. [38]. Suppose that we expand G in terms of the x-coordinate eigenfunctions, $\phi_n(x) = c_n \cos(\omega_n x)$, where $\omega_n = \frac{n\pi}{\eta_2}$ and $c_0 = 1/\sqrt{\eta_2}, c_n = \sqrt{2/\eta_2}$ for $n > 0$. That is,

$$G(\mathbf{r}, \mathbf{r}') = \sum_{n=0}^{\infty} \phi_n(x)\phi_n(x')H_n(y, y'). \tag{A.1}$$

Substitution into (3.7) yields the following equation for the y–dependent Green's functions H_n

$$\sum_{n=0}^{\infty} \phi_n(x)\phi_n(x')\frac{\partial^2 H_0(y, y')}{\partial y^2} + \sum_{n=1}^{\infty} \omega_n^2 \phi_n(x)\phi_n(x')H_n(y, y') = \frac{1}{|\Sigma|} - \delta(\mathbf{r} - \mathbf{r}'). \tag{A.2}$$

Taking inner products of both sides of the equation with eigenfunctions $\phi_m(x)$ then yields

$$\frac{\partial^2 H_0}{\partial y^2} = \frac{1}{\eta_1} - \delta(y - y') \tag{A.3}$$

$$\left(\omega_m^2 H_m(y, y') + \frac{\partial^2 H_m}{\partial y^2}\right)\phi_m(x') = -\delta(y - y')\phi_m(x'), \quad m \geq 1. \tag{A.4}$$

The generalized Green's function, H_0, is given by

$$H_0(y, y') = \frac{\eta_1}{3} + \frac{1}{2\eta_1}(y^2 + {y'}^2) - \max\{y, y'\}, \tag{A.5}$$

and the Green's functions for $n \geq 1$ are given by

$$H_n(y, y') = \frac{1}{\omega_n \sinh(\omega_n \eta_1)} \begin{cases} \cosh(\omega_n y)\cosh(\omega_n(\eta_1 - y')), & y < y' \\ \cosh(\omega_n(\eta_1 - y))\cosh(\omega_n y'), & y > y' \end{cases} \tag{A.6}$$

Combining these results, we have the full Neumann Green's function

$$G(\mathbf{r}, \mathbf{r}') = \frac{1}{\eta_2}H_0(y, y') + \frac{1}{\pi}\sum_{n=1}^{\infty} \cos\left(\frac{n\pi x}{\eta_2}\right)\cos\left(\frac{n\pi x'}{\eta_2}\right)\left(\frac{\cosh(\omega_n(\eta_1 - |y - y'|)) + \cosh(\omega_n(\eta_1 - |y + y'|))}{n\sinh(\omega_n\eta_1)}\right), \tag{A.7}$$

This incomplete eigenfunction expansion is useful for computing the logarithmic expansion of the Green's function. Writing $2\sinh(\omega_n\eta_1) = \mathrm{e}^{\pi/\eta_2}[1 - \mathrm{e}^{-2\pi/\eta_2}]$, we expand the denominator in a geometric series and express all other functions as exponentials to give

$$\begin{aligned} G(\mathbf{r}, \mathbf{r}') = \frac{1}{\eta_2}H_0(y, y') + \frac{1}{4\pi}\sum_{n=1}^{\infty}\sum_{j=0}^{\infty}\frac{1}{n}\tau^{nj}\tau^{n/2}\left(z_+^n + \bar{z}_+^n + z_-^n + \bar{z}_-^n\right) \\ \times\left(\tau^{-n/2}\zeta_-^n + \tau^{n/2}\zeta_-^{-n} + \tau^{-n/2}\zeta_+^n + \tau^{n/2}\zeta_+^{-n}\right), \end{aligned} \tag{A.8}$$

where

$$\tau = e^{-2\pi\eta_1/\eta_2}, \quad z_\pm = \mathrm{e}^{i\pi(x \pm x')/\eta_2}, \quad \zeta_\pm = e^{-\pi|y \pm y'|/\eta_2}, \quad \varsigma_\pm = e^{-\pi(2\eta_1 - |y \pm y'|)/\eta_2}. \tag{A.9}$$

Performing the series summation with respect to n finally gives the logarithmic series representation

$$G(\mathbf{r}, \mathbf{r}') = \frac{1}{\eta_2}H_0(y, y') - \frac{1}{2\pi}\sum_{j=0}^{\infty}\sum_{n=\pm}\sum_{m=\pm}\left(\log|1 - \tau^j z_n\zeta_m| + \log|1 - \tau^j z_n\varsigma_m|\right). \tag{A.10}$$

Appendix B

In this appendix we compute higher order terms in the QSS reduction of the CK equations (2.1) and (2.2) to the corresponding FP equation (2.20). For simplicity, we will assume that $\langle \mathbf{v} \rangle = 0$, $D_0 = 0$ and $\mathcal{Q}$ is chosen so that diffusion is isotropic. Define the asymptotic expansions

$$w(\mathbf{r}, \theta, t) \sim \sum_{j=0}^{n} \epsilon^j z_j(\mathbf{r}, \theta, t), \qquad w_0(\mathbf{r}, t) \sim \sum_{j=0}^{n} \epsilon^j \hat{z}_j(\mathbf{r}, t). \tag{B.1}$$

From equation (2.15) we have

$$\frac{\partial u}{\partial t} = -k\chi(\mathbf{r}) b u - \epsilon \sum_{j=0}^{n} \epsilon^j \left\langle \langle \mathbf{v} \cdot \nabla z_j \rangle \right\rangle - \epsilon k \chi(\mathbf{r}) \sum_{j=0}^{n} \epsilon^j \hat{z}_j. \tag{B.2}$$

We also have from (2.16)

$$\beta \sum_{j=0}^{n} \epsilon^j z_j - \alpha \mathcal{Q}(\theta) \sum_{j=0}^{n} \epsilon^j \hat{z}_j = -a\mathcal{Q}(\theta) \frac{\partial u}{\partial t} - a\mathcal{Q}(\theta) \mathbf{v}(\theta) \cdot \nabla u - \epsilon \sum_{j=0}^{n} \epsilon^j \frac{\partial z_j}{\partial t} - \epsilon \sum_{j=0}^{n} \epsilon^j \mathbf{v}(\theta) \cdot \nabla z_j. \tag{B.3}$$

Substituting (B.2) into (B.3) we have

$$\begin{aligned} \beta \sum_{j=0}^{n} \epsilon^j z_j - \alpha \mathcal{Q}(\theta) \sum_{j=0}^{n} \epsilon^j \hat{z}_j = a\mathcal{Q}(\theta) \left(b k \chi(\mathbf{r}) u - \mathbf{v}(\theta) \cdot \nabla u \right) + \epsilon a \mathcal{Q}(\theta) \left(\sum_{j=0}^{n} \epsilon^j \left\langle \langle \mathbf{v} \cdot \nabla z_j \rangle \right\rangle + k\chi(\mathbf{r}) \sum_{j=0}^{n} \epsilon^j \hat{z}_j \right) \\ - \epsilon \sum_{j=0}^{n} \epsilon^j \mathbf{v}(\theta) \cdot \nabla z_j - \epsilon \sum_{j=0}^{n} \epsilon^j \frac{\partial z_j}{\partial t}. \end{aligned} \tag{B.4}$$

Integrating (B.4) over θ provides a second equation

$$\begin{aligned} \beta \sum_{j=0}^{n} \epsilon^j \left\langle \langle z_j \rangle \right\rangle - \alpha \sum_{j=0}^{n} \epsilon^j \hat{z}_j = abk\chi(\mathbf{r}) u - \epsilon b \sum_{j=0}^{n} \epsilon^j \left\langle \langle \mathbf{v} \cdot \nabla z_j \rangle \right\rangle \\ + \epsilon a k \chi(\mathbf{r}) \sum_{j=0}^{n} \epsilon^j \hat{z}_j - \epsilon \sum_{j=0}^{n} \epsilon^j \frac{\partial \left\langle \langle z_j \rangle \right\rangle}{\partial t}. \end{aligned} \tag{B.5}$$

Equation (2.12) provides an additional constraint

$$\left\langle \langle z_j \rangle \right\rangle + \hat{z}_j = 0. \tag{B.6}$$

Combining (B.6) and (B.5) yields

$$\begin{aligned} (\alpha + \beta) \sum_{j=0}^{n} \epsilon^j \hat{z}_j = -abk\chi(\mathbf{r}) u + \epsilon b \sum_{j=0}^{n} \epsilon^j \left\langle \langle \mathbf{v} \cdot \nabla z_j \rangle \right\rangle \\ - \epsilon a k \chi(\mathbf{r}) \sum_{j=0}^{n} \epsilon^j \hat{z}_j + \epsilon \sum_{j=0}^{n} \epsilon^j \frac{\partial \left\langle \langle z_j \rangle \right\rangle}{\partial t}. \end{aligned} \tag{B.7}$$

Finally, substituting (B.7) into (B.4) yields

$$\begin{aligned} \beta \sum_{j=0}^{n} \epsilon^j z_j = a\mathcal{Q}(\theta) b^2 k \chi(\mathbf{r}) u - a\mathcal{Q}(\theta) \mathbf{v}(\theta) \cdot \nabla u + \epsilon a \mathcal{Q}(\theta)(b+1) \sum_{j=0}^{n} \epsilon^j \left\langle \langle \mathbf{v} \cdot \nabla z_j \rangle \right\rangle - \epsilon \sum_{j=0}^{n} \epsilon^j \mathbf{v}(\theta) \cdot \nabla z_j \\ + \epsilon a \mathcal{Q}(\theta) b k \chi(\mathbf{r}) \sum_{j=0}^{n} \epsilon^j \hat{z}_j + \epsilon \sum_{j=0}^{n} \epsilon^j \frac{\partial}{\partial t} \left(a\mathcal{Q}(\theta) \left\langle \langle z_j \rangle \right\rangle - z_j \right). \end{aligned} \tag{B.8}$$

Equations (B.7) and (B.8) generate a hierarchy of equations for z_j and $\hat{z}_j$. At leading order in ϵ we have

$$\hat{z}_0 = -\frac{1}{\beta} ab^2 k\chi(\mathbf{r})u \tag{B.9}$$

$$z_0 = \frac{a\mathcal{Q}(\theta)}{\beta}\left(b^2 k\chi(\mathbf{r})u - \mathbf{v}(\theta)\cdot\nabla u\right), \tag{B.10}$$

which are equivalent to equations (2.18) and (2.19) for $D_0 = 0$ and $\langle \mathbf{v}\rangle = 0$. To obtain higher order terms, we write z_j and $\hat{z}_j$ as

$$\hat{z}_j = \mu_j k\chi(\mathbf{r})u \tag{B.11}$$

$$z_j = \sigma_j \mathcal{Q}(\theta) k\chi(\mathbf{r})u + \varphi_j \mathcal{Q}(\theta)\mathbf{v}(\theta)\cdot\nabla u, \tag{B.12}$$

where μ_j, σ_j, and φ_j depend upon $\chi(\mathbf{r})$ but are otherwise independent of space and time. In doing so, we are neglecting higher spatial derivatives of u and terms that depend on $\langle \mathbf{v}\rangle$. From (B.9) and (B.10) we have that

$$\mu_0 = -\frac{1}{\beta} ab^2, \quad \sigma_0 = \frac{1}{\beta} ab^2, \quad \varphi_0 = -\frac{a}{\beta}. \tag{B.13}$$

In terms of the effective FP equation, the coefficients μ_j contribute to the detection rate, whereas the coefficients φ_j contribute to the diffusivity (assuming $\mathcal{Q}(\theta)$ is chosen so that diffusion is isotropic). More specifically,

$$\lambda \sim \lambda_0 + \epsilon k^2 \chi(\mathbf{r}) \sum_{j=0}^{n} \epsilon^j \mu_j, \quad D \sim \frac{\epsilon v^2}{2}\left(\frac{a}{\beta} - \sum_{j=1}^{n} \epsilon^j \varphi_j\right). \tag{B.14}$$

Although the σ_j terms only contribute to the drift velocity in the effective FP equation, they must still be computed in order to determine higher order coefficients μ_j and φ_j.

In order to complete our analysis, we still need to determine the term $\partial z_j/\partial t$ appearing on the right–hand side of equations (B.7) and (B.8). Differentiating equation (B.12) with respect to t and using (B.2) shows that

$$\begin{aligned}\frac{\partial z_j}{\partial t} &= \mathcal{Q}(\theta)\left[\sigma_j k\chi(\mathbf{r}) + \varphi_j \mathbf{v}(\theta)\cdot\nabla\right]\frac{\partial u}{\partial t} \\ &= -kb\chi(\mathbf{r})\mathcal{Q}(\theta)\left[\sigma_j k u + \varphi_j \mathbf{v}(\theta)\cdot\nabla u\right] \\ &\quad - \epsilon\mathcal{Q}(\theta)\left[\sigma_j k\chi(\mathbf{r}) + \varphi_j \mathbf{v}(\theta)\cdot\nabla\right]\left(\sum_{i=0}^{n}\epsilon^i \langle\langle \mathbf{v}\cdot\nabla z_i\rangle\rangle + k\chi(\mathbf{r})\sum_{i=0}^{n}\epsilon^i \hat{z}_i\right).\end{aligned} \tag{B.15}$$

Substituting for z_i and $\bar{z}_i$ on the right–hand side using (B.11) and (B.12), dropping higher order derivatives in space, and assuming $\langle \mathbf{v}\rangle = 0$ finally yields

$$\frac{\partial z_j}{\partial t} = -\mathcal{Q}(\theta)\sigma_j k\chi(\mathbf{r})\left(bk + \epsilon k^2 \sum_{i=0}^{n}\epsilon^i \mu_i\right)u - \mathcal{Q}\varphi_j\left(bk + \epsilon k^2\sum_{i=0}^{n}\epsilon^i\mu_i\right)\mathbf{v}(\theta)\cdot\nabla u. \tag{B.16}$$

Integrating the above equation with respect to θ and substituting the result for $\partial\langle\langle z_j\rangle\rangle/\partial t$ into (B.7) yields after some algebra

$$\beta\sum_{j=0}^{n}\epsilon^j\mu_j = -ab^2 - \epsilon b\sum_{j=0}^{n}\epsilon^j(ak\mu_j + bk\sigma_j) - \epsilon^2 bk^2\sum_{j=0}^{n}\sum_{i=0}^{n}\epsilon^{i+j}\sigma_j\mu_i. \tag{B.17}$$

Again we have used (B.11) and (B.12), dropped higher order derivatives in space, and set $\langle \mathbf{v}\rangle = 0$. Similarly, using equations (B.11), (B.12) and (B.16), we find that equation (B.8) reduces to the form

$$\begin{aligned}\beta\sum_{j=0}^{n}\epsilon^j\left(\sigma_j k\chi(\mathbf{r})u + \varphi_j\mathbf{v}(\theta)\cdot\nabla u\right) &= -\left(a - \epsilon k\chi(\mathbf{r})\sum_{j=0}^{n}\epsilon^j(b\varphi_j - \sigma_j) - \epsilon^2 k^2\chi(\mathbf{r})\sum_{j=0}^{n}\sum_{i=0}^{n}\epsilon^{i+j}\varphi_j\mu_i\right)\mathbf{v}(\theta)\cdot\nabla u \\ &\quad + \left(ab^2 + \epsilon b\sum_{j=0}^{n}\epsilon^j(ak\mu_j + bk\sigma_j) + \epsilon^2 bk^2\sum_{j=0}^{n}\sum_{i=0}^{n}\epsilon^{i+j}\sigma_j\mu_i\right)k\chi(\mathbf{r})u,\end{aligned} \tag{B.18}$$

which results in the u-independent pair of equations

$$\beta\sum_{j=0}^{n}\epsilon^j\sigma_j = ab^2 + \epsilon b\sum_{j=0}^{n}\epsilon^j(ak\mu_j + bk\sigma_j) + \epsilon^2 bk^2\sum_{j=0}^{n}\sum_{i=0}^{n}\epsilon^{i+j}\sigma_j\mu_i, \tag{B.19}$$

$$\beta\sum_{j=0}^{n}\epsilon^j\varphi_j = -a + \epsilon k\chi(\mathbf{r})\sum_{j=0}^{n}\epsilon^j(b\varphi_j - \sigma_j) + \epsilon^2 k^2\chi(\mathbf{r})\sum_{j=0}^{n}\sum_{i=0}^{n}\epsilon^{i+j}\varphi_j\mu_i. \tag{B.20}$$

Notice that (B.19) and (B.17) imply that $\sigma_j = -\mu_j$, for all $j = 0, 1, \cdots, n$. Substituting this into (B.17) and (B.20) yields

$$\beta\sum_{j=0}^{n}\epsilon^j\mu_j = -ab^2 - \epsilon bk(a-b)\sum_{j=0}^{n}\epsilon^j\mu_j + \epsilon^2 bk^2\sum_{j=0}^{n}\sum_{i=0}^{n}\epsilon^{i+j}\mu_j\mu_i, \tag{B.21}$$

$$\beta\sum_{j=0}^{n}\epsilon^j\varphi_j = -a + \epsilon k\chi(\mathbf{r})\sum_{j=0}^{n}\epsilon^j(b\varphi_j + \mu_j) + \epsilon^2 k^2\chi(\mathbf{r})\sum_{j=0}^{n}\sum_{i=0}^{n}\epsilon^{i+j}\varphi_j\mu_i. \tag{B.22}$$

Collecting $\mathcal{O}(\epsilon)$ terms we have

$$\mu_1 = -\frac{1}{\beta}bk(a-b)\mu_0 = \frac{a}{\beta^2}(a-b)b^3k \tag{B.23}$$

$$\varphi_1 = \frac{1}{\beta}k\chi(\mathbf{r})(b\varphi_0 + \mu_0) = -\frac{a}{\beta^2}b(b+1)k\chi(\mathbf{r}). \tag{B.24}$$

For $\mathcal{O}(\epsilon^n)$, $n \geq 2$, the recursion becomes nonlinear, with

$$\mu_n = -\frac{1}{\beta}\left(bk(a-b)\mu_{n-1} - bk^2\sum_{j=0}^{n-2}\mu_j\mu_{n-j-2}\right), \tag{B.25}$$

$$\varphi_n = \frac{\chi(\mathbf{r})}{\beta}\left(k(b\varphi_{n-1} + \mu_{n-1}) + k^2\sum_{j=0}^{n-2}\varphi_j\mu_{n-j-2}\right). \tag{B.26}$$

[1] J. W. Bell, Searching Behaviour, The Behavioural Ecology of Finding Resources (London: Chapman and Hall, 1991) .

[2] G. M. Viswanathan, V. Afanasyev, S. V. Buldyrev, E. J. Murphy, H. A. Prince and H. E. Stanley, Nature **381**, 413 (1996).

[3] G. M. Viswanathan, S. V. Buldyrev, S. Havlin, M. G. E. da Luz, E. P. Raposo and H. E. Stanley, Nature, **401**, 911 (1999).

[4] F. Bartumeus, J. Catalan, U. L. Fulco, M. L. Lyra and G. M. Viswanathan, Phys. Rev. Lett., **88**, 097901 (2002).

[5] A. Caspi, R. Granek and M. Elbaum, Phys. Rev. E **66**, 011916 (2002).

[6] D. Arcizet, B. Meier, E. Sackmann, J. O. Radler and D. Heinrich, Phys. Rev. Lett. **101**, 248103 (2002).

[7] S. Klumpp and R. Lipowsky, Phys. Rev. Lett. **95**, 268102 (2005).

[8] O. Bénichou, C. Loverdo, M. Moreau, and R. Voituriez. *Phys. Rev. E*, **74** 020102 (2006).

[9] C. Loverdo, O. Benichou, M. Moreau and R. Voituriez, Nature Phys. **4**, 134 (2008).

[10] A. Kahana, G. Kenan, M. Feingold, M. Elbaum and R. Granek, Phys. Rev. E **78**, 051912 (2008).

[11] O. G. Berg and C. Blomberg, Biophys. Chem. **4**, 367 (1976).

[12] S. E. Halford and J. F. Marko. Nucleic Acids Res., **32** 3040 (2004).

[13] M. Slutsky and L. A. Mirny, Biophys. J, **87** 1640; 4021 (2004).

[14] M. Coppey, O. Benichou, R. Voituriez and M. Moreau, Biophys. J. **87**, 1640 (2004).

[15] C. R. Bramham and D. G. Wells, Nat. Rev. Neurosci.**8**, 776 (2007).

[16] P. C. Bressloff and J. Newby, New J. Phys. **11**, 023033 (2009).

[17] J. Newby and P. C. Bressloff Phys. Rev. E. **80**, 021913 (2009).

[18] O. Benichou, M. Coppey, M. Moreau, P. H. Suet and R. Voituriez, Phys. Rev. Lett. **19**, 198101 (2005).

[19] O. Benichou, M. Coppey, M. Moreau, P. H. Suet and R. Voituriez, J. Cond. Matt **17**, S4275S4286 (2005).

[20] O. Benichou, C. Loverdo, M. Moreau and R. Voituriez,

J. Phys. Cond. Matt. **19**, 065141 (2007).
[21] C. Loverdo, O. Benichou, M. Moreau and R. Voituriez, Phys. Rev. E **80**, 031146 (2009).
[22] O. Bénichou, C. Loverdo, M. Moreau, and R. Voituriez. Intermittent search strategies. *Rev. Mod. Phys.*, **83** 81 (2011).
[23] Rook M S, Lu M and Kosik K S *J. Neurosci.* **20** 6385–6393 (2000)
[24] J. L. Dynes and O. Steward, J. Comp. Neurol. **500**, 433 (2007).
[25] M. Welte, Curr. Biol. **14** R525 (2004).
[26] C. Kural, H. Kim, S. Seyd, G. Goshima, V. I. Gelfand and P. R. Selvin, Science **308**, 1469 (2005).
[27] M. J. Muller, S. Klumpp and R. Lipowsky, Proc. Natl. Acad. Sci. U. S. A. **105** 4609 (2008).
[28] M. J. Muller, S. Klumpp and R. Lipowsky, J. Stat. Phys. **133** 1059 (2008).
[29] J. Newby and P. C. Bressloff, Bull. Math. Biol. **72**, 1840 (2010).
[30] J. Newby and P. C. Bressloff, J. Stat. Mech. **P04014**, (2010).
[31] J. Newby and P. C. Bressloff, Phys. Biol.. **7**, 036004 (2010).
[32] L. Goldstein and Z. Yang, Ann. Rev. Neurosci.**23**, 39 (2000).
[33] B. Alberts, A. Johnson, J. Lewis, M. Raff, K. Roberts and P. Walter, Molecular Biology of the Cell, 5th Ed. (Garland, New York, 2008) .
[34] E. M. Damm and L. Pelkmans, Cell Microbiol. **8**, 1219 (2006).
[35] T. Lagache, E. Dauty and D. Holcman, Curr. Opin. Microbiol. **12**, 439 (2009).
[36] H. Salman, A. Abu-Arish, S. Oliel, A. Loyter, J. Klafter, R. Granek and M. Elbaum, Biophys. J. **89**, 2134 (2005).
[37] M. J. Ward. *Natural Resource Modeling*, 13(2):271–302, 2000.
[38] S. Pillay, M. J. Ward, A. Peirce, and T. Kolokolnikov. *Multiscale Modeling and Simulation*, 8(3):803–835, 2010.
[39] A. F. Cheviakov, M. J. Ward, and R. Straube. *Multiscale Modeling and Simulation*, 8(3):836–870, 2010.
[40] C. W. Gardiner. *Handbook of stochastic methods for physics, chemistry, and the natural sciences*, Springer-Verlag, Berlin (1983).
[41] S. Redner, A Guide to First Passage Time Processes (Cambridge: Cambridge University Press, 2001) .
[42] A. N. Becalska and E. R. Gavis. *Development* **136** 2493 (2009).
[43] V. L. Zimyanin . *et. al.*. *Cell* **134** 843 (2008).

RECENT REPORTS

56/10	The Influence of Bioreactor Geometry and the Mechanical Environment on Engineered Tissues	Osborne ODea Whiteley Byrne Waters
57/10	A numerical guide to the solution of the bidomain equations of cardiac electrophysiology	Pathmanathan Bernabeu Bordas Cooper Garny Pitt-Francis Whiteley Gavaghan
58/10	Particle-scale structure in frozen colloidal suspensions from small angle X-ray scattering	Spannuth Mochrie Peppin Wettlaufer
59/10	Spin coating of an evaporating polymer solution	Munch Please Wagner
60/10	Stochastic synchronization of neuronal populations with intrinsic and extrinsic noise	Bressloff Lai
61/10	Metastable states and quasicycles in a stochastic Wilson-Cowan model of neuronal population dynamics	Bressloff
62/10	Adsorption and desorption dynamics of citric acid anions in soil	Oburger Leitner Jones Zygalakis Schnepf Roose
63/10	A dual porosity model of nutrient uptake by root hairs soil	Zygalakis Kirk Jones Roose Wissuwa
64/10	Hot Charge Pairs and Charge Generation in Donor Acceptor Blends	Kirkpatrick
65/10	Excluded-volume effects in the diffusion of hard spheres	Bruna Chapman
66/10	Dynamics of colloidal particles in ice	Spannuth Mochrie Peppin Wettlaufer
01/11	Improving the efficiency of optical coherence tomography by using the non-ideal behaviour of a polarising beam splitter	Lippok Nielsen Vanholsbeeck
02/11	Self-diffusion in remodelling and growth	Epstein

06/11	A numerical methodology for the Painleve equations	Fornberg Weideman
07/11	Strong stability preserving two-step Runke-Kutta methods	Ketcheson Gotlieb MacDonald
08/11	Hysteresis and Post Walrasian Economics	Cross McNamara Kalachev Pokrovskii
09/11	A locally adaptive time-stepping algorithm for petroleum reservoir simulations	McNamara Bowen Dellar
10/11	On the predictions and limitations of the BeckerDoring model for reaction kinetics in micellar surfactant solutions	Griffiths Bain Breward Colegate Howell Waters
11/11	Dynamics of the Tear Film	Braun
12/11	The infuence of receptor-mediated interactions on reaction-diffusion mechanisms of cellular self-organisation	Klikaa Baker Headon Gaffney

Copies of these, and any other OCCAM reports can be obtained from:

Oxford Centre for Collaborative Applied Mathematics
Mathematical Institute
24 - 29 St Giles'
Oxford
OX1 3LB
England
www.maths.ox.ac.uk/occam